Adaptive DKT Finite Element for Plate Bending Analysis

Bhothikhun P.

Department of Mechanical Engineering, Faculty of Engineering, Chulalongkorn University, Bangkok, Thailand

Dechaumphai P.

Department of Mechanical Engineering, Faculty of Engineering, Chulalongkorn University, Bangkok, Thailand
E-mail address: fmepdc@eng.chula.ac.th

Abstract

Discrete Kirchhoff Triangle (DKT) which provides high solution accuracy for plate bending analysis combined with adaptive meshing technique is presented. The DKT plate bending finite element formulation with detailed finite element matrices are derived. Performance of the DKT element is evaluated by comparing with the exact solution. An adaptive meshing technique is applied to generate small elements in the regions of high stress gradient to improve the computed solutions. Larger elements are generated in the other regions to reduce the problem unknowns and thus the computational time. The effectiveness of the combined method is evaluated by several problems. Results show that the combined method can improve the solution accuracy and reduce the computational effort.

Keywords*: finite element, plate bending, Discrete Kirchhoff Triangle, adaptive mesh*

1 Introduction

The finite element method has been widely used for the analysis of plate bending problems. Different types of plate bending elements have been developed during the past decades to improve the sufficiency and solution accuracy [1]. One of the element types which provide high solution accuracy for the analysis of plate bending problem is the Discrete Kirchhoff Triangle (DKT) [2]. With the advantages of the three-node triangular element that can provide high flexibility in the construction of finite models for complex geometry and can easily be combined with an adaptive meshing technique [3-5] to provide high solution accuracy at reduced computational effort, the three-node triangular DKT element is studied in this paper in order to combine with an adaptive meshing technique to improve the overall analysis solution accuracy.

In this paper, detailed formulation and the corresponding finite element matrices of the DKT element are presented. The performance of the DKT element will be evaluated by problems that have exact or analytical solutions. The adaptive meshing technique presented herein generates small elements in the regions of high stress gradients to provide higher solution accuracy. Meanwhile, larger elements are generated in the other regions to reduce the total number of unknowns and the computational time. Because the technique generates appropriate element sizes automatically, it is thus suitable for complex problems where a priori knowledge of the solutions does not exist.

The governing differential equations for the transverse deflection of plate will be presented first. Then, the corresponding finite element equations and element matrices will be derived and presented. The basic concepts of the adaptive meshing technique and the selection of the meshing parameters used for constructing new meshes will be explained. Finally, the performance of the DKT element and the adaptive meshing technique are evaluated by analyzing several examples.

2 Governing Equations

The equation for the transverse deflection, w, in the z-direction normal to the x-y plane of a thin plate, with

a constant thickness of t whose middle plane is coincident with the x-y plane, is given by the equilibrium equation in the form [6],

$$D\left(\frac{\partial^4 w}{\partial x^4}+\frac{\partial^4 w}{\partial x^2\partial y^2}+\frac{\partial^4 w}{\partial y^4}\right) = p(x,y) \quad (1)$$

where $p(x,y)$ is the applied lateral load normal to the plate and D is the bending rigidity which is defined by,

$$D = \frac{Et^3}{12(1-\nu^2)} \quad (2)$$

where E is the modulus of elasticity, t is the thickness of the plate and ν is the Poisson's ratio.

3 Finite Element Equations

The derivation of the three-node DKT element equations is based on the following assumptions [2]: 1) both the x- and y-twist angles vary quadratically over the element, 2) the transverse shears are zero at the tip nodes, 3) the transverse deflection is in form of a cubic function over the element, and 4) the twist angles normal to the element sides vary linearly. The finite element equations are derived by applying the method of weighted residuals to the plate bending equation Eq. (1) leading to the finite element equations in the form,

$$[K]\{\delta\} = \{F\} \quad (3)$$

where the vector $\{\delta\}$ contains the element nodal unknowns of the transverse deflections and the rotations. The unknowns of each node are a transverse deflection in the element local z-coordinate direction and two rotations about the element local x-y coordinate directions. Thus there are nine degrees of freedom per element. The element stiffness matrix, $[K]$, and the nodal force vector due to the applied loads, $\{F\}$, are defined by,

$$[K] = \int_A [B]^T [D][B]\, dA \quad (4)$$

$$\{F\} = \int_A [N]^T p\, dA \quad (5)$$

where the strain-displacement interpolation matrix, $[B]$, is defined by,

$$[B]=\frac{1}{2A}\begin{bmatrix} y_{31}\left[\frac{\partial H_x}{\partial \xi}\right]+y_{12}\left[\frac{\partial H_x}{\partial \eta}\right] \\ -x_{31}\left[\frac{\partial H_y}{\partial \xi}\right]-x_{12}\left[\frac{\partial H_y}{\partial \eta}\right] \\ -x_{31}\left[\frac{\partial H_x}{\partial \xi}\right]-x_{12}\left[\frac{\partial H_x}{\partial \eta}\right]+y_{31}\left[\frac{\partial H_y}{\partial \xi}\right]+y_{12}\left[\frac{\partial H_y}{\partial \eta}\right] \end{bmatrix} \quad (6)$$

$$\left\{\frac{\partial H_x}{\partial \xi}\right\}=\begin{Bmatrix} P_6(1-2\xi)+\eta(P_5-P_6) \\ q_6(1-2\xi)-\eta(q_5+q_6) \\ -4+6(\xi+\eta)+r_6(1-2\xi)-\eta(r_5+r_6) \\ -P_6(1-2\xi)+\eta(P_4+P_6) \\ q_6(1-2\xi)+\eta(q_4-q_6) \\ -2+6\xi+r_6(1-2\xi)+\eta(r_4-r_6) \\ -\eta(P_4+P_5) \\ \eta(q_4-q_5) \\ \eta(r_4-r_5) \end{Bmatrix} \quad (7)$$

$$\left\{\frac{\partial H_y}{\partial \xi}\right\}=\begin{Bmatrix} t_6(1-2\xi)+\eta(t_5-t_6) \\ 1+r_6(1-2\xi)-\eta(r_5+r_6) \\ -q_6(1-2\xi)+\eta(q_5+q_6) \\ -t_6(1-2\xi)+\eta(t_4+t_6) \\ -1+r_6(1-2\xi)+\eta(r_4-r_6) \\ -q_6(1-2\xi)-\eta(q_4-q_6) \\ -\eta(t_4+t_5) \\ \eta(r_4-r_5) \\ -\eta(q_4-q_5) \end{Bmatrix} \quad (8)$$

$$\left\{\frac{\partial H_x}{\partial \eta}\right\}=\begin{Bmatrix} -P_5(1-2\eta)+\xi(P_5-P_6) \\ q_5(1-2\eta)-\xi(q_5+q_6) \\ -4+6(\xi+\eta)+r_5(1-2\eta)-\xi(r_5+r_6) \\ \xi(P_4+P_6) \\ \xi(q_4-q_6) \\ \xi(r_4-r_6) \\ P_5(1-2\eta)-\xi(P_4+P_5) \\ q_5(1-2\eta)+\xi(q_4-q_5) \\ -2+6\eta+r_5(1-2\eta)+\xi(r_4-r_5) \end{Bmatrix} \quad (9)$$

$$\left\{\frac{\partial H_y}{\partial \eta}\right\}=\begin{Bmatrix} -t_5(1-2\eta)+\xi(t_5-t_6) \\ 1+r_5(1-2\eta)-\xi(r_5+r_6) \\ -q_5(1-2\eta)+\xi(q_5+q_6) \\ \xi(t_4+t_6) \\ \xi(r_4-r_6) \\ -\xi(q_4-q_6) \\ t_5(1-2\eta)-\xi(t_4+t_5) \\ -1+r_5(1-2\eta)+\xi(r_4-r_5) \\ -q_5(1-2\eta)-\xi(q_4-q_5) \end{Bmatrix} \quad (10)$$

The coefficients P_k, q_k, r_k and t_k, k = 4, 5, 6 depend on the element shape and are given by,

$$P_k=\frac{-6x_{ij}}{\ell_{ij}^2} \quad (11)$$

$$q_k=\frac{3x_{ij}y_{ij}}{\ell_{ij}^2} \quad (12)$$

$$r_k=\frac{3y_{ij}^2}{\ell_{ij}^2} \quad (13)$$

$$t_k=\frac{-6y_{ij}}{\ell_{ij}^2} \quad (14)$$

$$\ell_{ij}=\sqrt{x_{ij}^2+y_{ij}^2} \quad (15)$$

where the coefficients x_{ij} and y_{ij}, $i, j = 1, 2, 3$ are defined in terms of element nodal coordinates by,

$$x_{ij}=x_i-x_j \quad (16)$$

$$y_{ij}=y_i-y_j \quad (17)$$

The matrix $[D]$ in Eq. (4) is the plate material stiffness matrix defined by,

$$[D] = \frac{Et^3}{12(1-\nu^2)}\begin{bmatrix} 1 & \nu & 0 \\ \nu & 1 & 0 \\ 0 & 0 & \frac{1-\nu}{2} \end{bmatrix} \quad (18)$$

The above finite element matrices are in closed-form so that they can be implemented in the computer program directly [7].

4 Adaptive Meshing Technique

4.1 *Adaptive Meshing concept*

The basic idea of adaptive meshing [4] is to construct a completely new mesh based on the solution obtained from the previous calculation. The new mesh will have small elements in regions of large changes in solution gradients and large elements in regions where the gradient changes are small. Suitable nodal spacings used for constructing a new mesh are determined by using the solid mechanics concept of finding the principal stresses, σ_1 and σ_2, from a given state of stresses, σ_x, σ_y and τ_{xy}, i.e.,

$$\begin{bmatrix} \sigma_x & \tau_{xy} \\ \tau_{xy} & \sigma_y \end{bmatrix} \Rightarrow \begin{bmatrix} \sigma_1 & 0 \\ 0 & \sigma_2 \end{bmatrix} \quad (19)$$

At a typical node in the previous mesh, the second derivatives of the key parameter for meshing, ϕ, (analogous to the stress components in Eq. (19)) are computed and the two eigenvalues (analogous to the principal stresses) are then determined,

$$\begin{bmatrix} \frac{\partial^2\phi}{\partial x^2} & \frac{\partial^2\phi}{\partial x\partial y} \\ \frac{\partial^2\phi}{\partial x\partial y} & \frac{\partial^2\phi}{\partial y^2} \end{bmatrix} \Rightarrow \begin{bmatrix} \lambda_1 & 0 \\ 0 & \lambda_2 \end{bmatrix} \quad (20)$$

The larger eigenvalue, $\lambda=\max(\lambda_1,\lambda_2)$, is then selected for that node and the same process is repeated for all the other nodes. Proper nodal spacings, denoted by h, used for constructing a new mesh are then determined from the condition required to procedure an optimal mesh;

$$\lambda h^2 = \text{constant} = \lambda_{\max} h_{\min}^2 \quad (21)$$

where $\lambda_{\max}$ is the largest eigenvalue of all nodes in the previous mesh and $h_{\min}$ is the specified minimum nodal spacing for the new mesh.

4.2 *Meshing Parameters*

The adaptive meshing technique requires a selection of proper key parameters (ϕ in Eq. (20)). For plate bending analysis, the Von Mises stress is used as a key parameter which is defined by,

$$\sigma_{Von\ Mises}=\frac{1}{\sqrt{2}}\sqrt{(\sigma_x-\sigma_y)^2+\sigma_x^2+\sigma_y^2+6\tau_{xy}^2} \quad (22)$$

5 Applications

Three example problems are presented in this section. The first example is chosen to evaluate the performance of the DKT plate bending element. The other two examples demonstrate the effectiveness of the adaptive meshing technique combining with the DKT element as presented below.

5.1 *Partially loaded simply supported square plate*

A square 2×2 m simply supported plate with a thickness of 0.01 m, subjected to a partially distributed load of 1 kN/m^2, is shown in Figure 1. The plate is assumed to have the modulus of elasticity of 7.2×10^{10} N/m^2 and the Poisson's ratio of 0.25. The exact transverse deflection can be derived [8] and is given by,

$$w=\frac{4pa^4}{D\pi^5}\sum_{m=1,3,5,\ldots}^{\infty}\frac{(-1)^{(m-1)/2}}{m^5}\sin\frac{m\pi u}{2a}\left\{1-\frac{\cosh\frac{m\pi y}{a}}{\cosh\alpha_m}\right.$$

$$\left[\cosh(\alpha_m-2\gamma_m)+\gamma_m\sinh(\alpha_m-2\gamma_m)+\alpha_m\frac{\sinh2\gamma_m}{2\cosh\alpha_m}\right]$$

$$\left.+\frac{\cosh(\alpha_m-2\gamma_m)}{2\cosh\alpha_m}\frac{m\pi y}{a}\sinh\frac{m\pi y}{a}\right\}\sin\frac{m\pi x}{a} \qquad (23)$$

Due to symmetry, a quarter of the plate is analyzed. The result of the transverse deflection obtained from the DKT element is shown in Figure 2. Figure 3 shows the predicted transverse deflections along the *x*-direction obtained from the DKT element as compared to the exact solution. The figure shows good comparison of the two solutions.

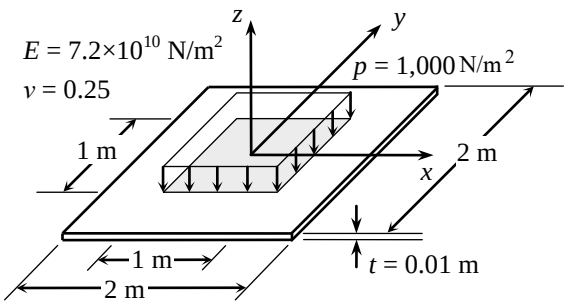

Figure 1: Problem statement of a simply supported square plate subjected to a partially distributed load.

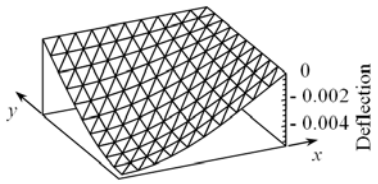

Figure 2: Predicted deflection of the plate using DKT plate bending element.

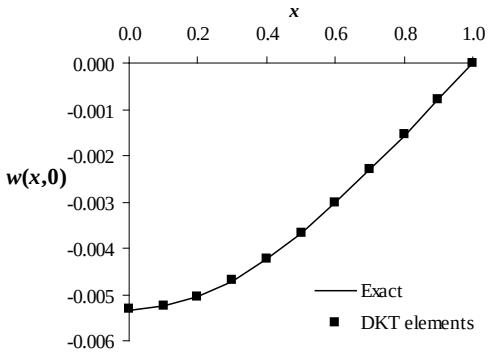

Figure 3: Comparative transverse deflections along *x*-direction from DKT finite element model with the exact solution.

5.2 *Simply supported square plate with circular hole*

A square $2b\times2b$ (3×3 m) simply supported plate which has a circular hole, radius of *R*, at the center and the thickness of 0.01 m is subjected to a uniform distributed load of 1,000 N/m^2 as shown in Figure 4. The plate is assumed to have the modulus of elasticity of 1.9×10^{11} N/m^2 and the Poisson's ratio of 0.3. The sizes of the circular hole of R/b = 1/6, 2/6, 3/6 and 4/6 are studied herein.

Firstly, the plate with the hole size of R/b = 1/6 is considered. Due to symmetry, an upper right quarter of the plate is analyzed. The model is discretized into 910 elements and 486 nodes as shown in Figure 5. Similarly, the plates with the hole size of R/b = 2/6, 3/6 and 4/6 are then considered with the model consisting of 285 nodes and 522 elements, 276 nodes and 504 elements, and 361 nodes and 204 elements respectively. The predicted transverse deflections in dimensionless form along the circular hole are compared with the analytical solution by Lo and Leissa [9] in Figure 6. The figure shows that the DKT element can provide good solution accuracy.

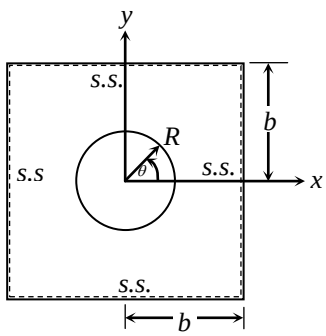

Figure 4: A simply supported square plate with circular hole.

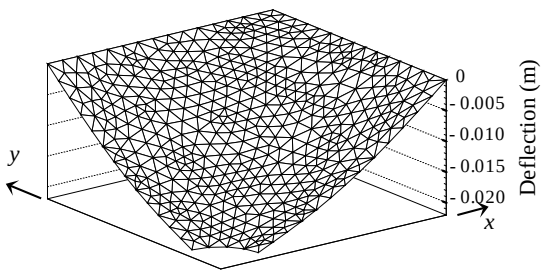

Figure 5: Predicted deformation of plate with circular hole using DKT element

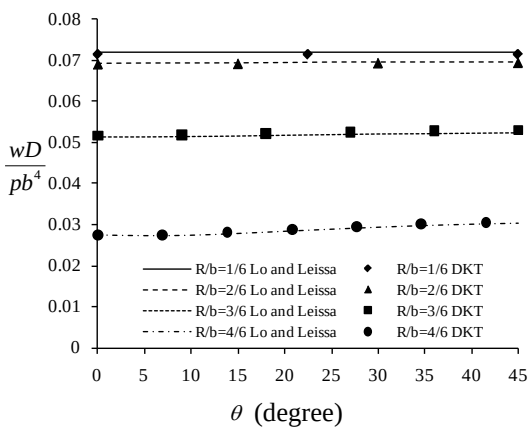

Figure 6: Transverse deflections along the hole obtained from the DKT element compared with the analytical solution.

The plate with the hole size R/b = 1/6 is reconsidered to evaluate the performance of the adaptive meshing technique. The model consisting of coarse mesh of 84 nodes and 142 elements as shown in Figure 7(a) is used for the initial calculation. The Von Mises stresses obtained from this initial mesh solution are used as the key parameter to generate a new mesh. The new adaptive mesh, with 155 nodes and 268 elements, is shown in Figure 7(b). The same process is applied to generate the second and third adaptive meshes. The second adaptive mesh with 267 nodes and 471 elements and the third adaptive mesh with 388 nodes and 694 elements are shown in Figure 7(c) and 7(d), respectively. Small elements are generated in the region of high stress gradients near the edge of the circular hole in order to increase the solution accuracy. The uniform fine mesh model with 1,521 nodes and 2,922 elements as shown in Figure 8 is also analyzed. The percentage errors of the maximum transverse deflections from both methods are shown in Figure 9. The results indicate that the adaptive meshing technique provides the same solution accuracy as compared to the finer mesh but with fewer numbers of unknowns. The Von Mises stress contours obtained from the third adaptive mesh and the fine mesh are also shown in Figure 10(a-b).

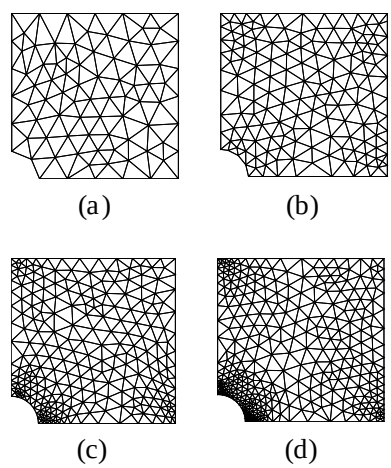

Figure 7: DKT finite element meshes: (a) initial mesh, (b) 1st adaptive mesh, (c) 2nd adaptive mesh and (d) 3rd adaptive mesh.

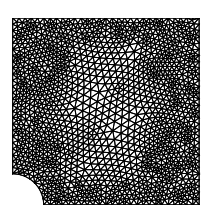

Figure 8: The fine DKT finite element model.

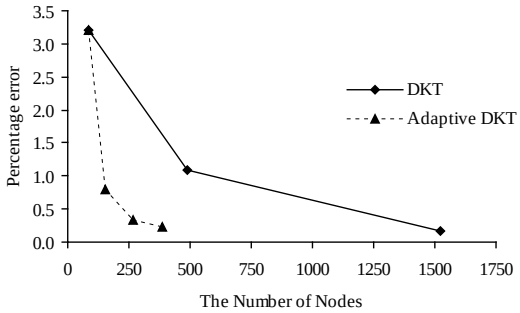

Figure 9: Comparative percentage errors of the plate maximum transverse deflections obtained from the adaptive and uniform meshes.

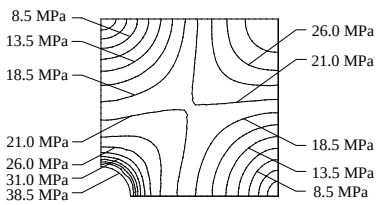

(a)

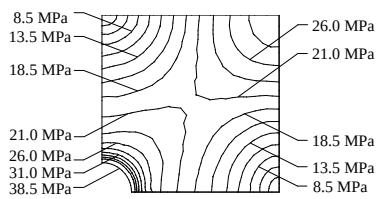

(b)

Figure 10: Predicted Von Mises stress contours of the plate: (a) 3rd adaptive mesh and (b) fine mesh.

5.3 *Plate with narrow cut subjected to vertical loading*

The problem statement of the plate with narrow cut subjected to vertical loading is shown in Figure 11. The plate is subjected to the uniform vertical load p = 1 kN/m along one edge of the plate. The initial mesh consists of 299 nodes and 543 elements as shown in Figure 12(a). The Von Mises stresses obtained from this initial mesh solution are used as the key parameter for the adaptive remeshing. The new adaptive mesh, with 849 nodes and 1604 elements, is shown in Figure 12(b). Small elements are generated in the region of high stress gradients near the end of the cutout to provide more accurate stress solution. The second adaptive mesh with 1493 nodes and 2846 elements and the third adaptive mesh with 1953 nodes and 3734 elements are shown in Figure 12(c) and 12(d), respectively. The figures show more refined elements are created in that region to capture the high stress concentration in order to increase the solution accuracy.

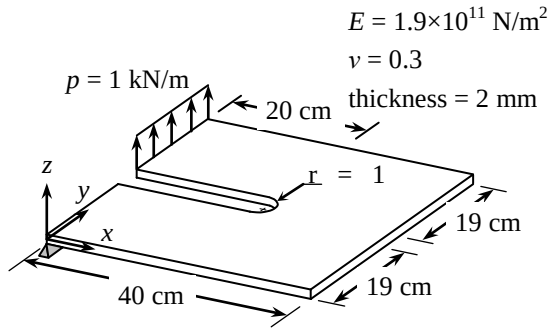

Figure 11: Problem statement of a plate with narrow cut subjected to vertical loading.

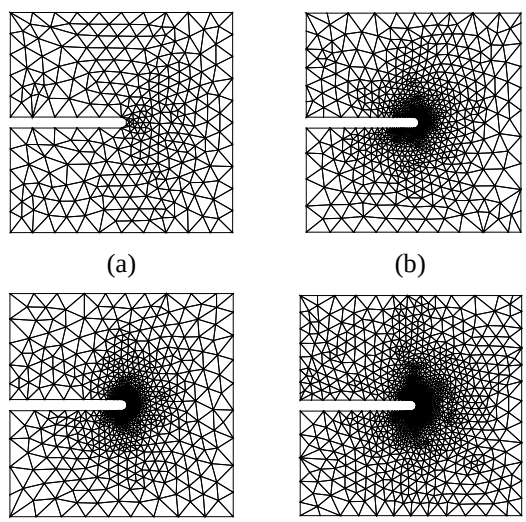

Figure 12: DKT finite element meshes: (a) initial mesh, (b) 1st adaptive mesh, (c) 2nd adaptive mesh, and (d) 3rd adaptive mesh.

Figure 13 shows that the predicted maximum Von Mises stress converges to the value of 2.40 GPa with the increase of the refined elements in the high stress concentration region. The deflection of the plate and the Von Mises stress contours by using the third adaptive finite element mesh are also shown in Figure 14 and Figure 15 respectively. Details of the Von Mises stress contours near the intense stress location are presented in Figure 16.

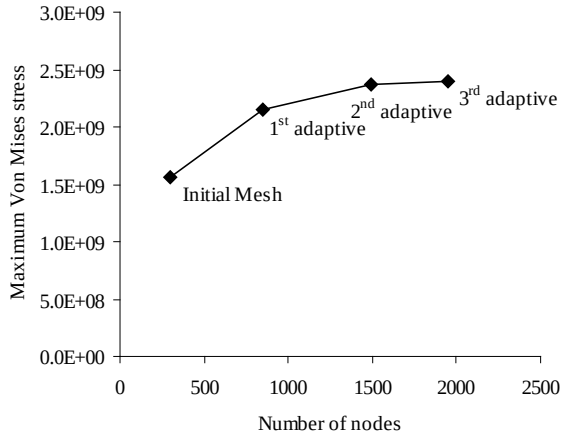

Figure 13: The convergence of predicted maximum Von Mises stress by using DKT adaptive finite element mesh.

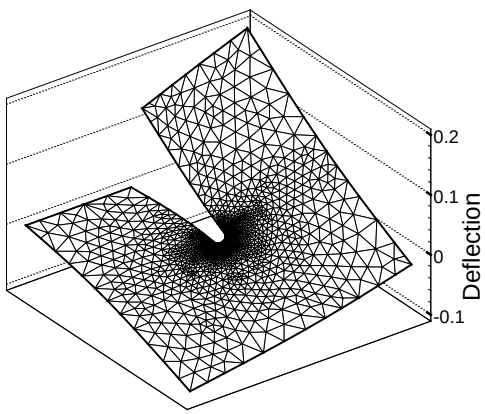

Figure 14: Predicted deflection of the plate using DKT 3rd adaptive finite element mesh.

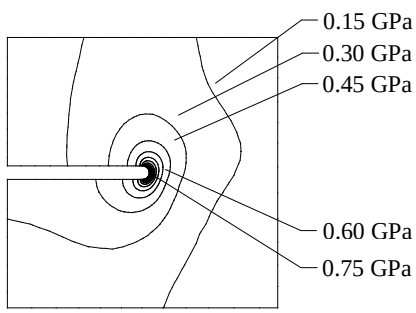

Figure 15: Predicted Von Mises stress contours of the plate using DKT 3rd adaptive finite element mesh.

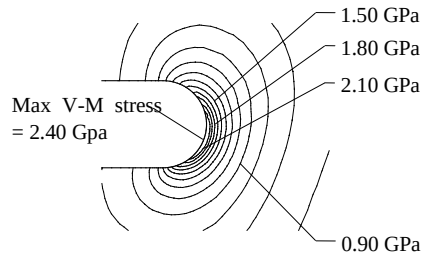

Figure 16: Predicted Von Mises stress contours of the plate using DKT 3rd adaptive finite element mesh in the region of high stresses.

6 Conclusions

The Discrete Kirchhoff Triangle (DKT) element was presented and evaluated by simple plate bending problem which has exact solution. The result indicated that the DKT element provides high solution accuracy.

An adaptive meshing technique combined with the DKT finite element for plate bending analysis was presented. The DKT plate bending element has been combined with the adaptive meshing technique to improve the solution accuracy and reduce the computational effort. The examples presented in this paper demonstrated that the adaptive meshing technique: (1) reduces modeling effort because a priori knowledge of the solution is not required; (2) provides high solution accuracy by adapting the mesh to the physics of the solutions; (3) reduces the total number of unknowns by automatically generating small elements in the regions with high solution gradients and large elements in the other regions.

References

[1] Hrabok M. M. and Hrudey T. M., 1984. A Review and Catalogue of Plate Bending Finite Elements, *Computers & Structures*, 19: 479-495.

[2] Batoz J. L., Bathe K. J., and Ho L. W., 1980. A Study of Three-Node Triangular Plate Bending Elements, *International Journal for Numerical Methods in Engineering*, 15: 1771-1812.

[3] Dechaumphai P., 1996. Improvement of Plane Stress Solutions Using Adaptive Finite Elements, *Journal of the Chinese Institute of Engineers*, 19(3): 375-380.

[4] Phongthanapanich S. and Dechaumphai P., 2009. Finite Element/Finite Volume Methods with Educational CAE Software, *AIJSTPME*, 2(1): 89-98.

[5] Traivivatana S., Phongthanapanich S. and Dechaumphai P., 2009. Finite Element/Finite Volume Methods with Educational CAE Software, *AIJSTPME*, 2(4): 21-31.

[6] Zienkiewicz O. C. and Taylor R. L., 2005. *The Finite Element Method for Solid and Structural Mechanics*, 6th Edition, Elsevier Butterworth-Heinemann, Oxford.

[7] Jeyachandrabose C., Kirkhope J. and Babu C. R., 1985. An Alternative Explicit Formulation for the DKT Plate-Bending Element, *International Journal for Numerical Methods in Engineering*, 21: 1289-1293.

[8] Timoshenko S. and Krieger S. W., 1970. *Theory of Plates and Shells*, 3rd Ed., McGraw-Hill, Singapore.

[9] Lo C. C. and Leissa A. W., 1966. Bending of Plates with Circular Holes, *Acta Mechanica*, 4: 64-78.